Supporting Information

Secondary Metabolites with Agricultural Antagonistic Potentials from *Beauveria felina*, a Marine-derived Entomopathogenic Fungus

Feng-Yu Du,[†,‡] Xiao-Ming Li,[†] Ze-Chun Sun,[‡] Ling-Hong Meng,[†] and Bin-Gui Wang[†,§,*]

[†]Key Laboratory of Experimental Marine Biology, Institute of Oceanology, Chinese Academy of Sciences, and Laboratory of Marine Biology and Biotechnology, Qingdao National Laboratory for Marine Science and Technology, Nanhai Road 7, Qingdao 266071, China

[‡]College of Chemistry and Pharmacy, Qingdao Agricultural University, Changcheng Road 700, Qingdao 266109, China

[§]Center for Ocean Mega-Science, Chinese Academy of Sciences, Nanhai Road 7, Qingdao 266071, China

Content

Figure S1. HR-ESI-MS spectrum of compound **1**.

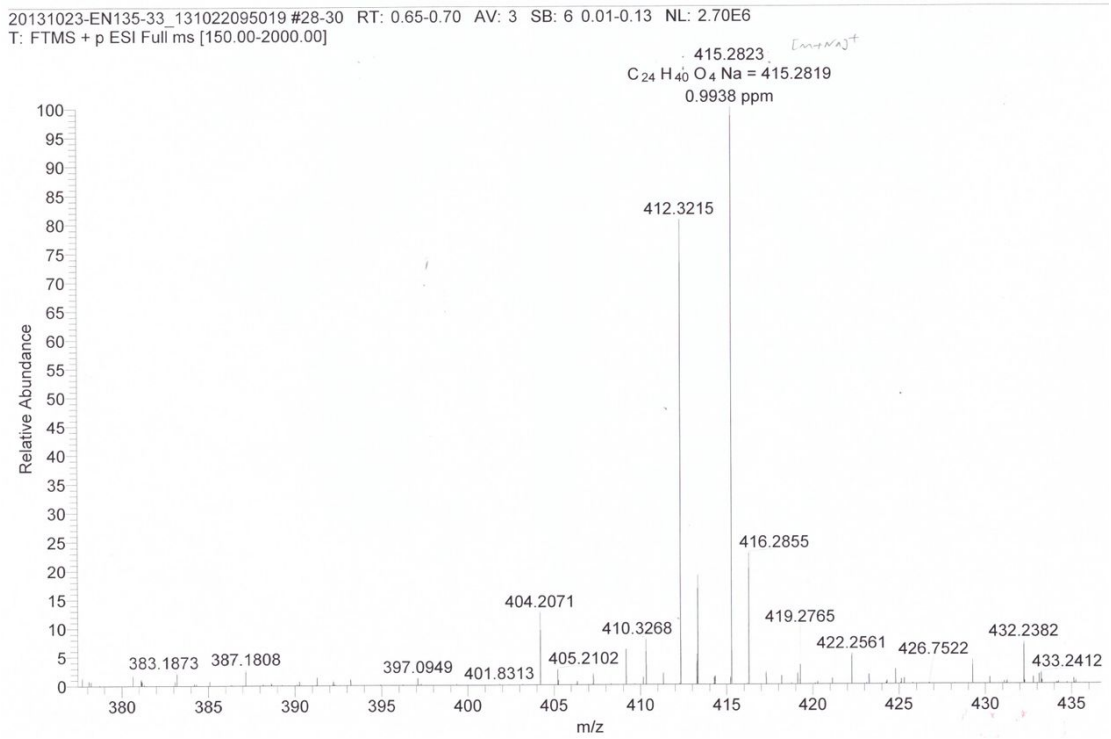

Figure S2. ^{1}H NMR (500 MHz, DMSO-d_6) spectrum of compound **1**.

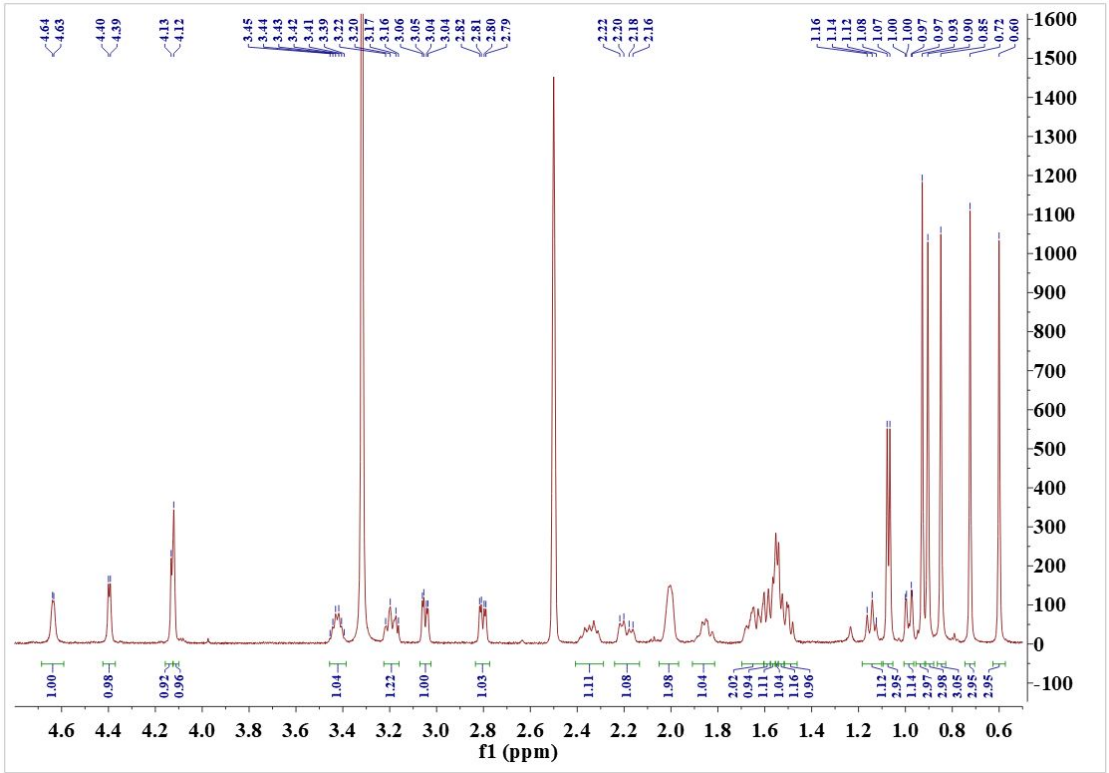

Figure S3. ^{13}C NMR (125 MHz, DMSO-d_6) and DEPT spectra of compound **1**.

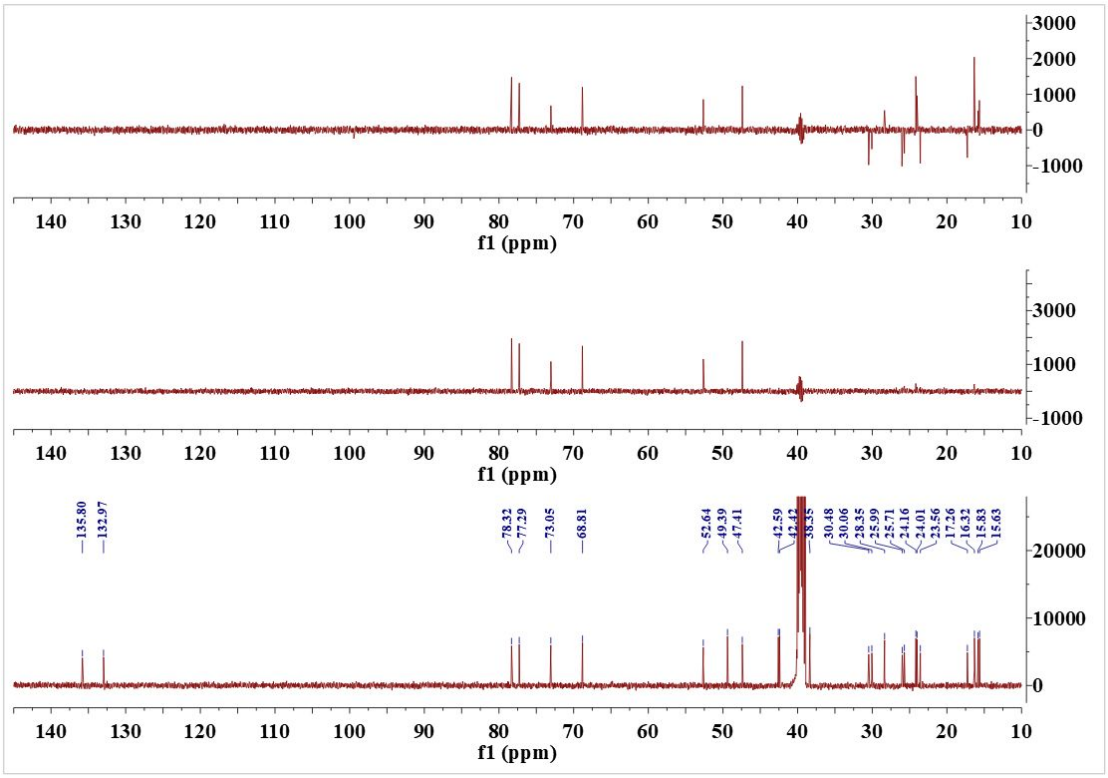

Figure S4. ^{1}H-^{1}H COSY spectrum of compound **1**.

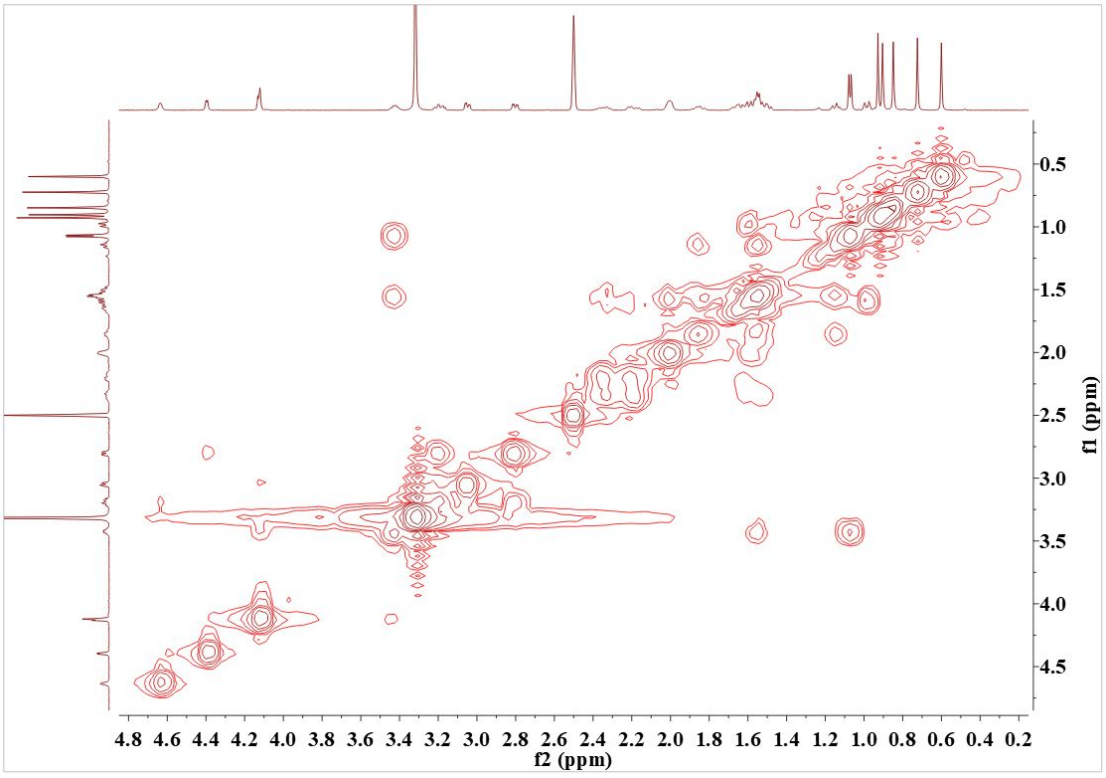

Figure S5. HSQC spectrum of compound **1**.

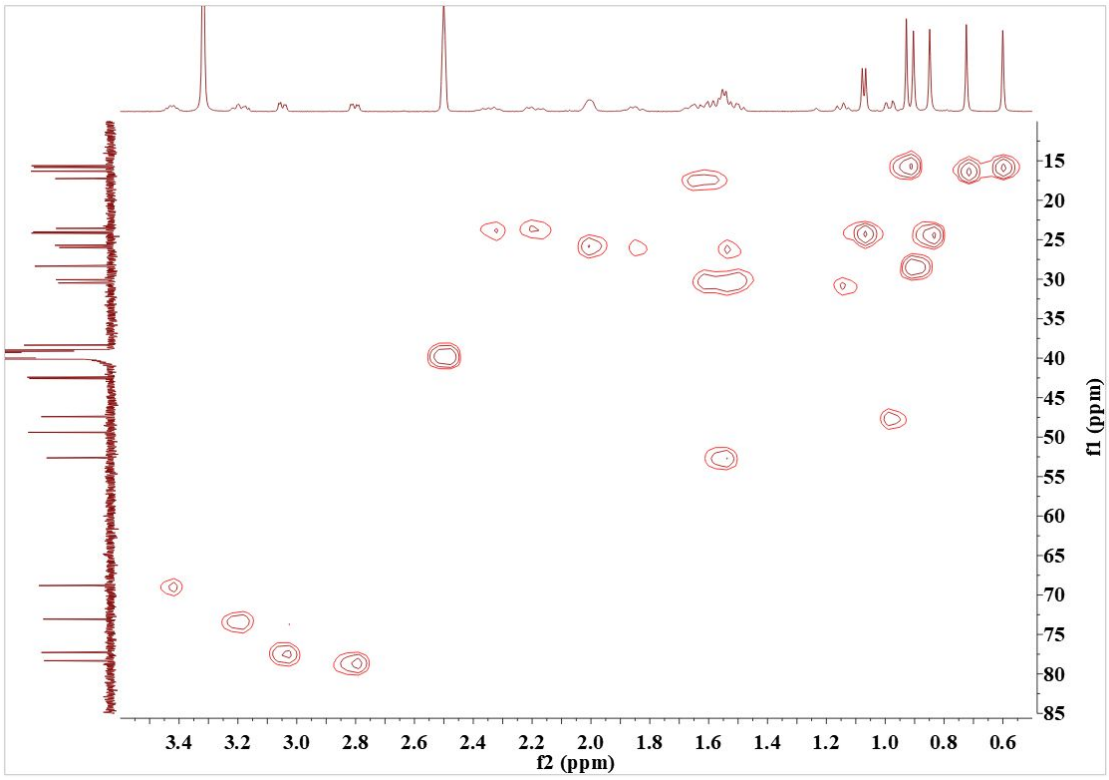

Figure S6. HMBC spectrum of compound **1**.

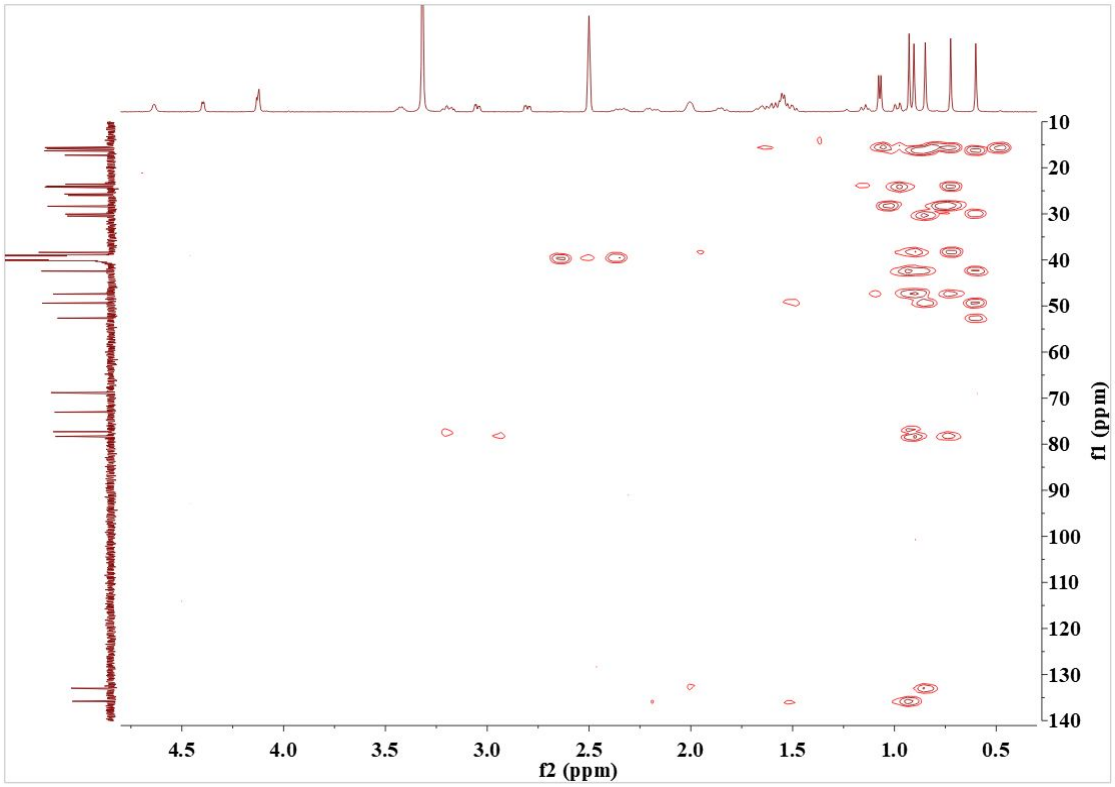

Figure S7. NOESY spectrum of compound **1**.

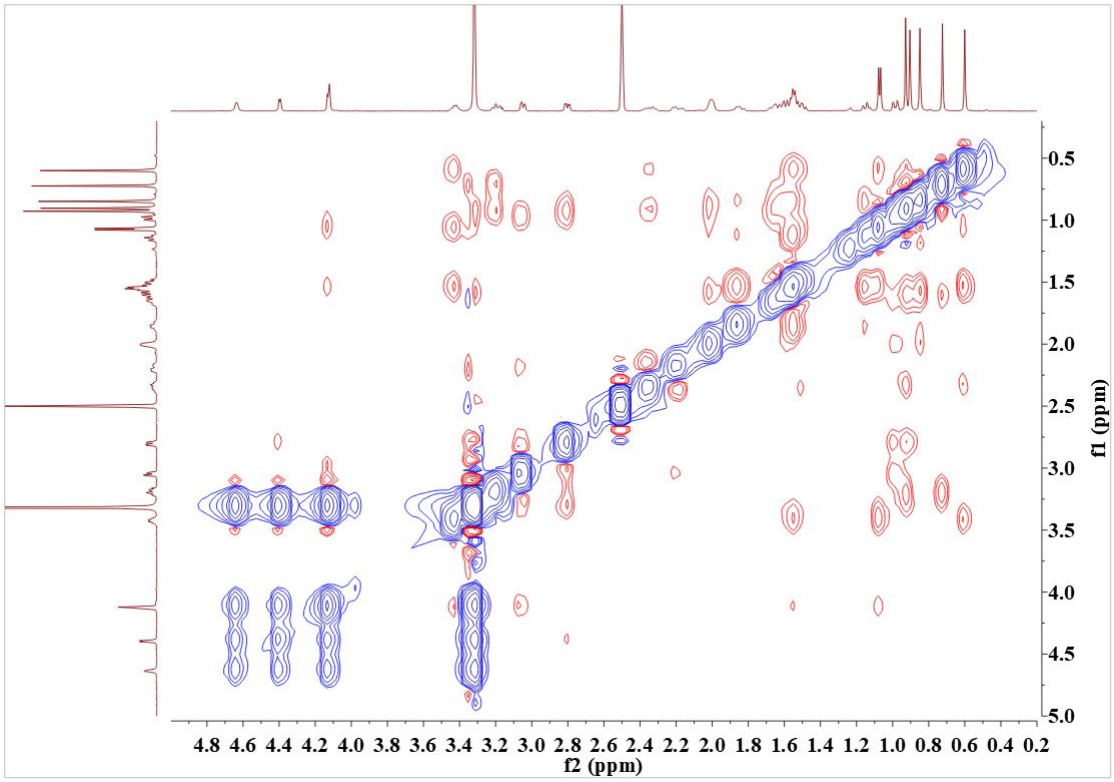

Figure S8. HR-ESI-MS spectrum of compound **2**.

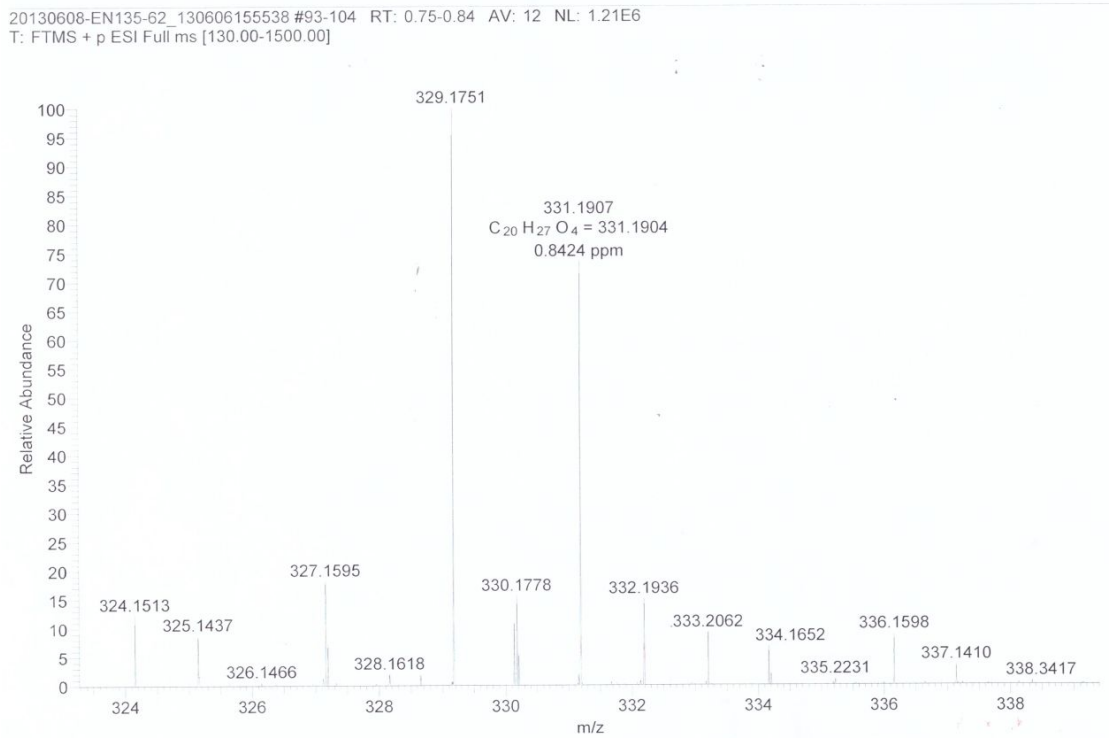

Figure S9. ^{1}H NMR (500 MHz, acetone-d_6) spectrum of compound **2**.

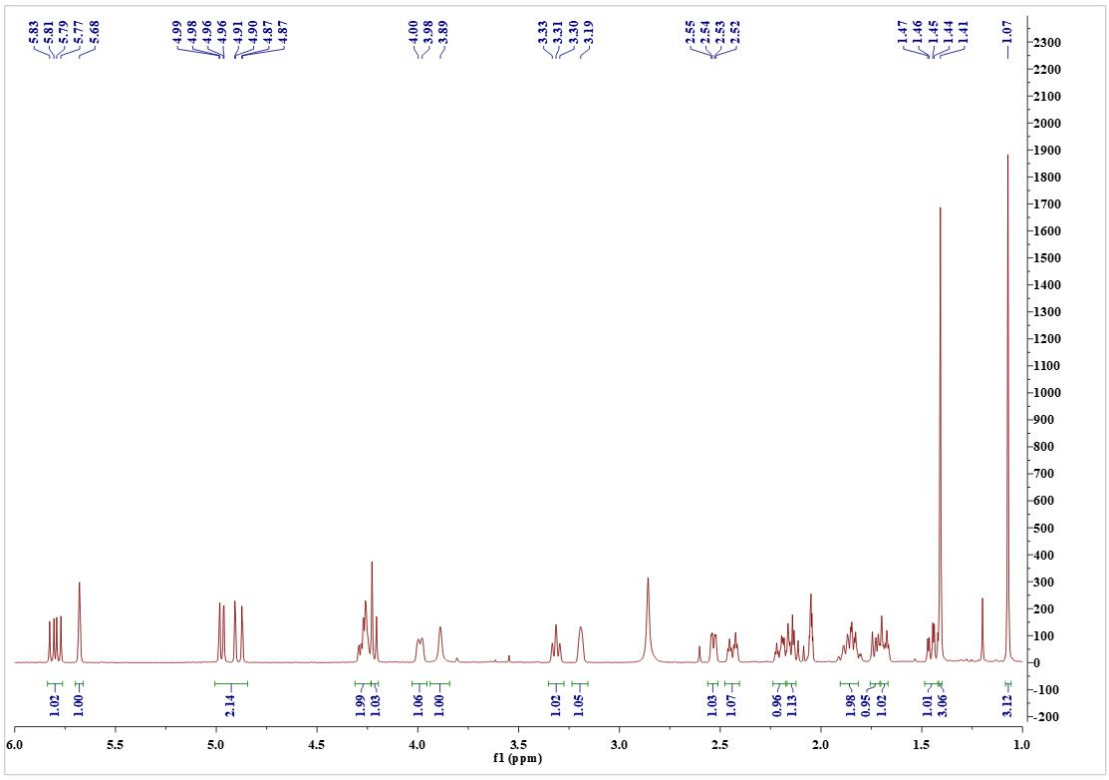

Figure S10. ^{13}C NMR (125 MHz, acetone-d_6) and DEPT spectra of compound **2**.

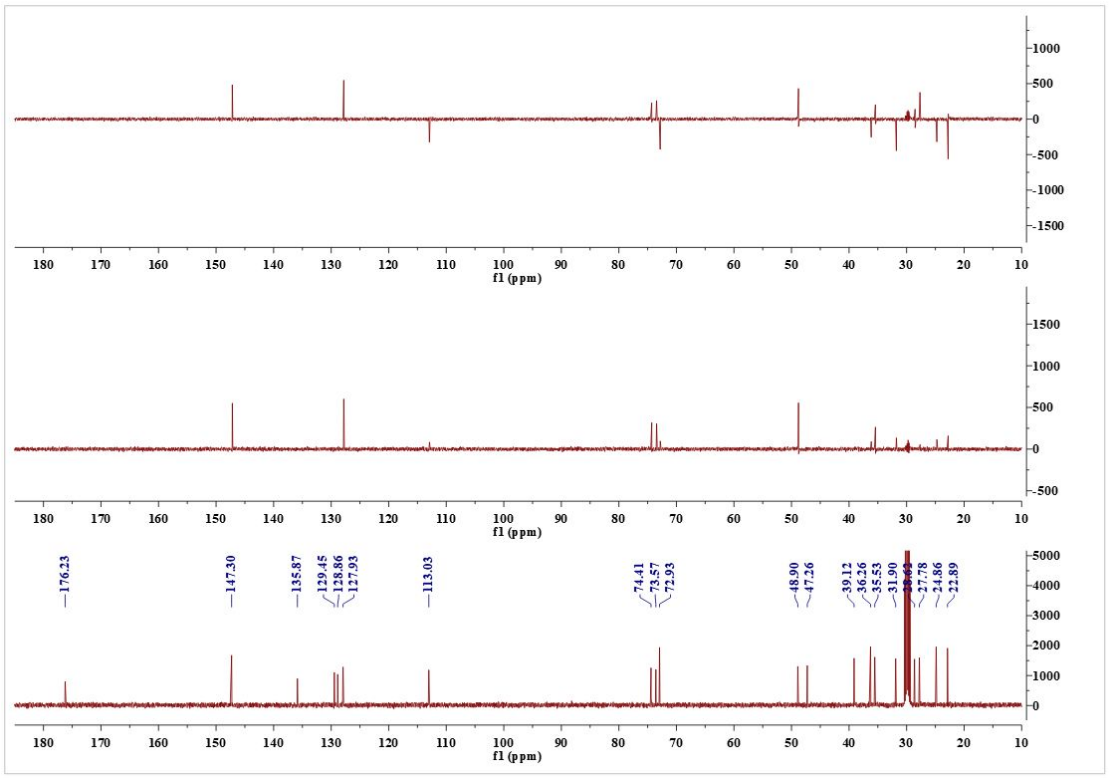

Figure S11. ^{1}H-^{1}H COSY spectrum of compound **2**.

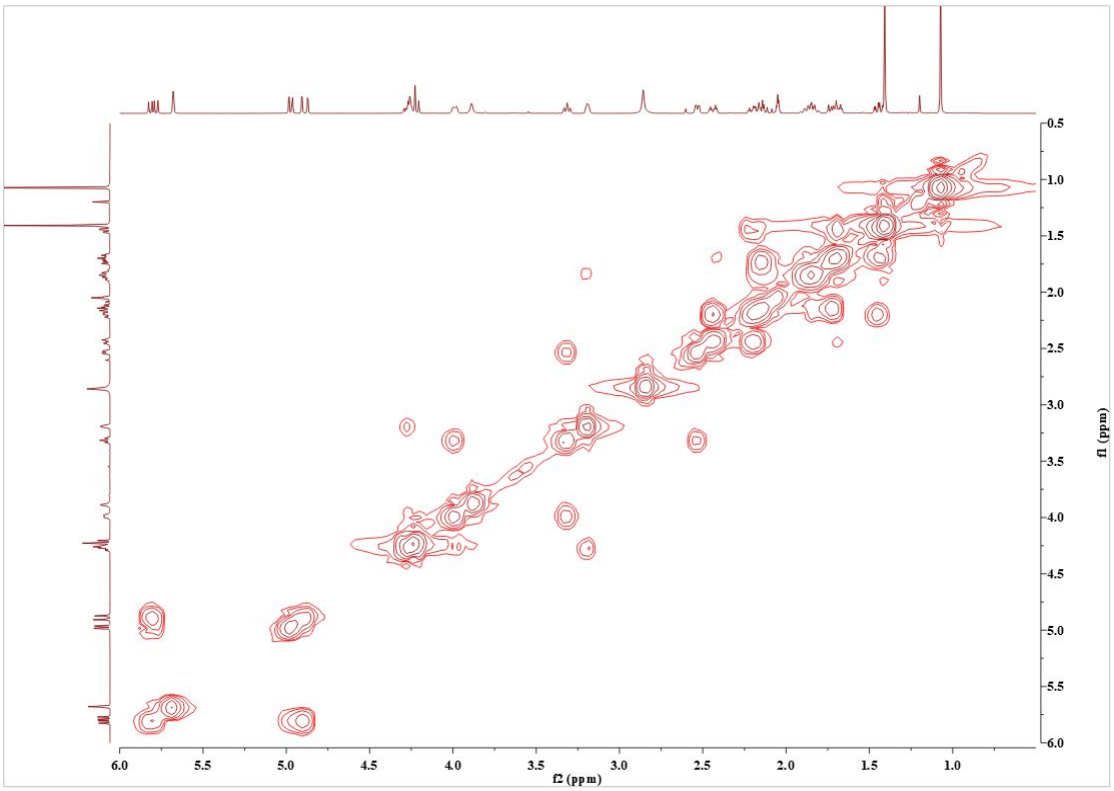

Figure S12. HSQC spectrum of compound **2**.

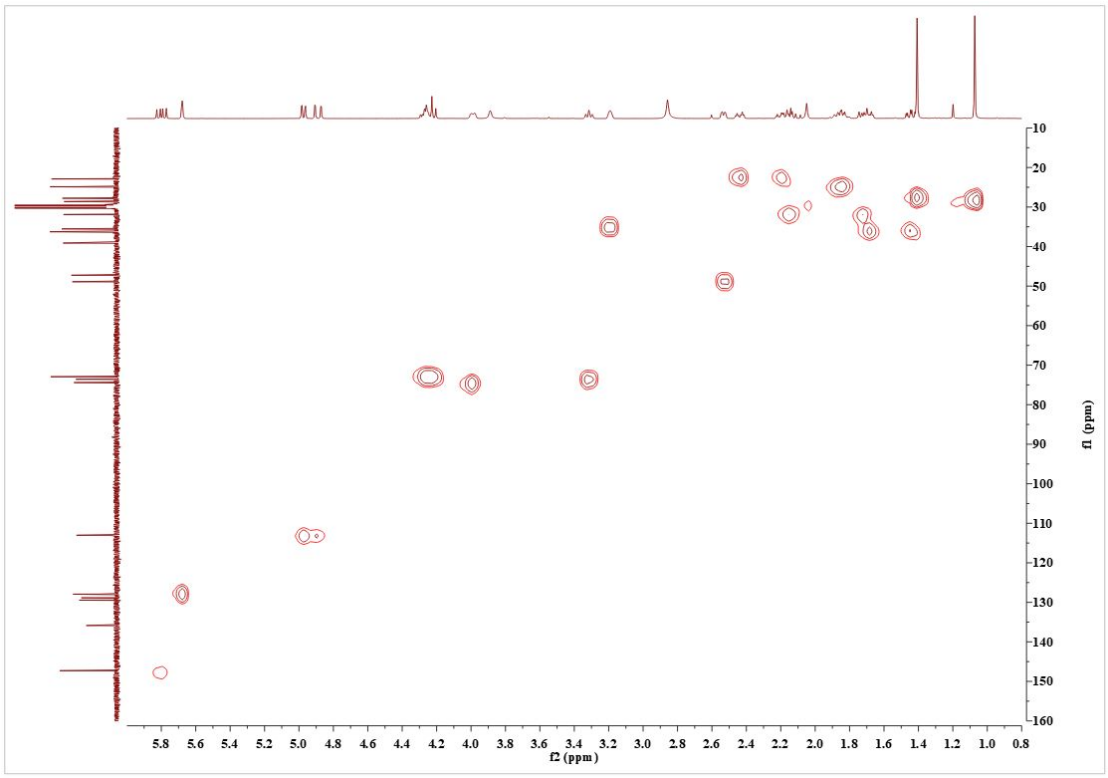

Figure S13. HMBC spectrum of compound **2**.

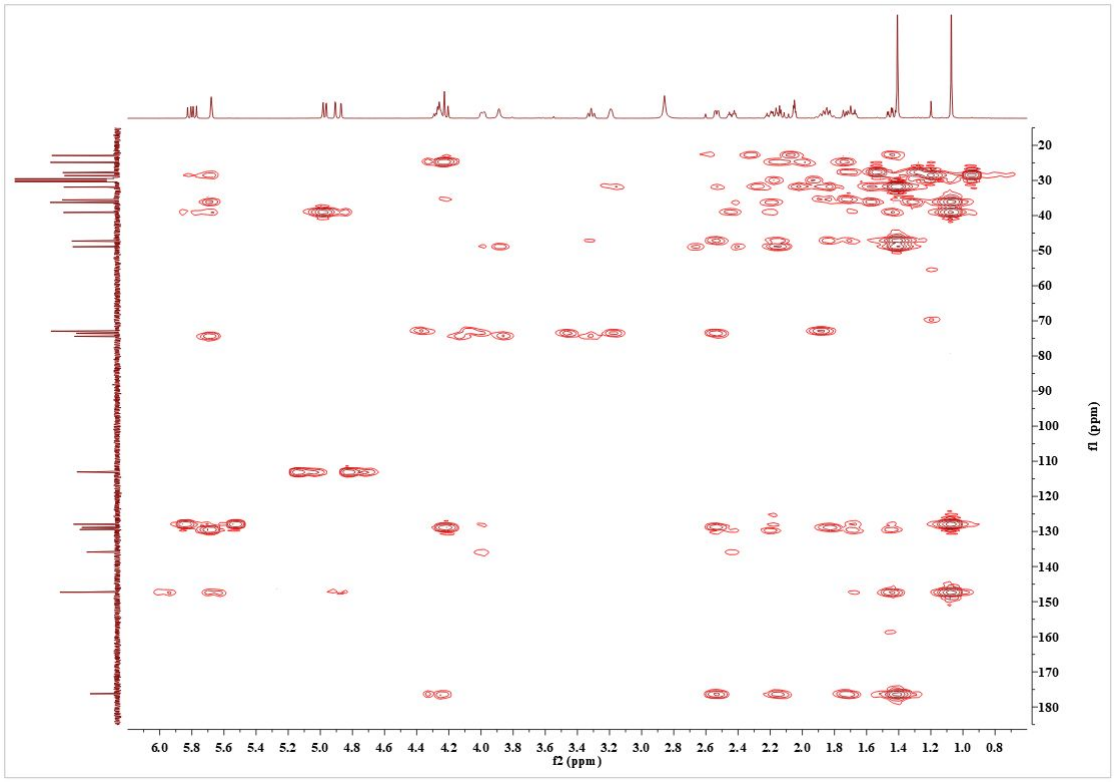

Figure S14. NOESY spectrum of compound **2**.

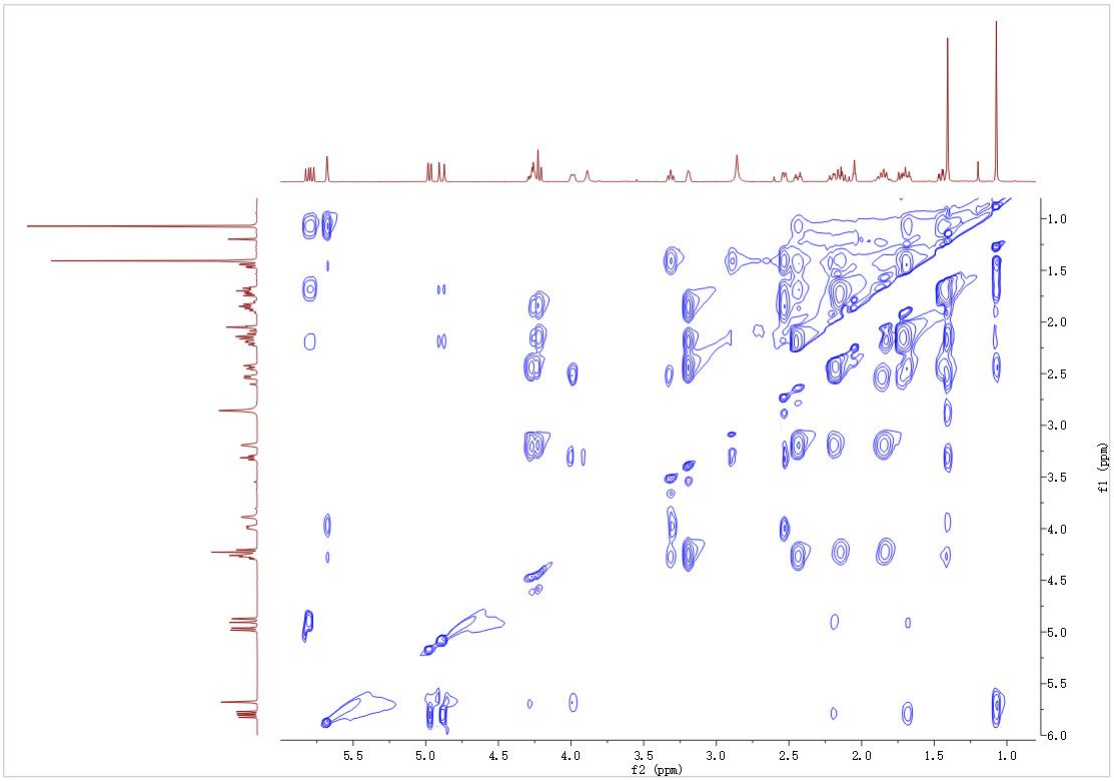

Figure S15. HR-ESI-MS spectrum of compound **3**.

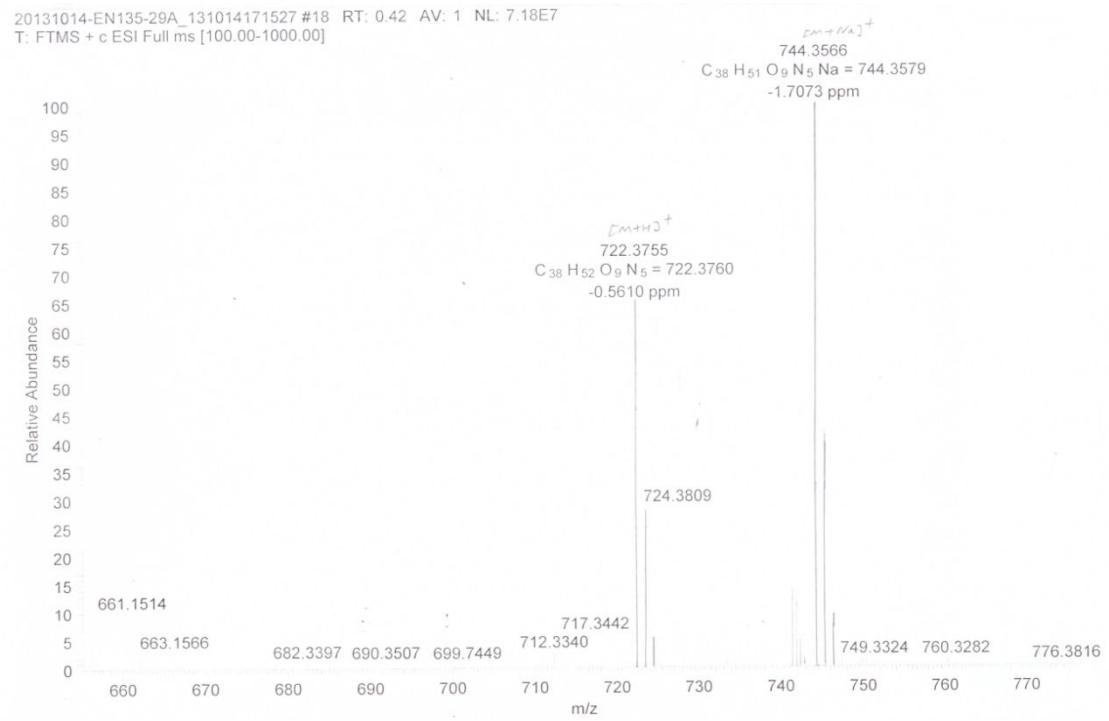

Figure S16. ^{13}C NMR (125 MHz, acetone-d_6) of compound **3**.

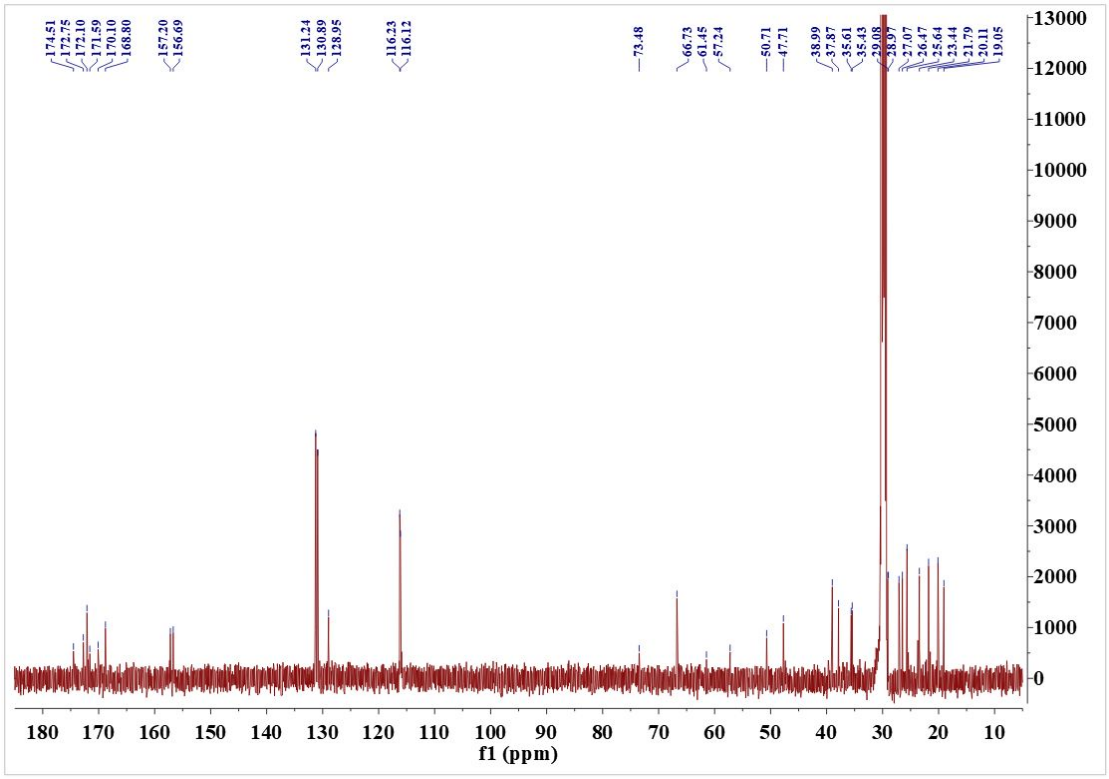

Figure S17. DEPT spectra of compound **3**.

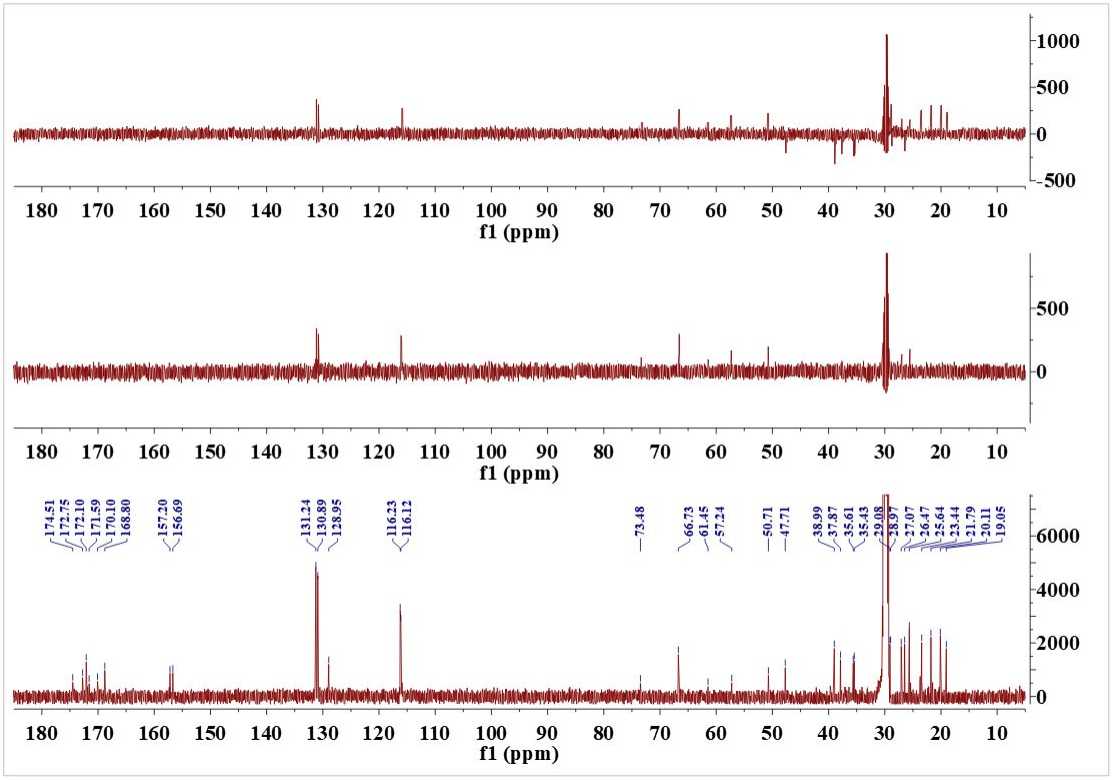

Figure S18. ^{1}H NMR (500 MHz, acetone-d_6) spectrum of compound **3**.

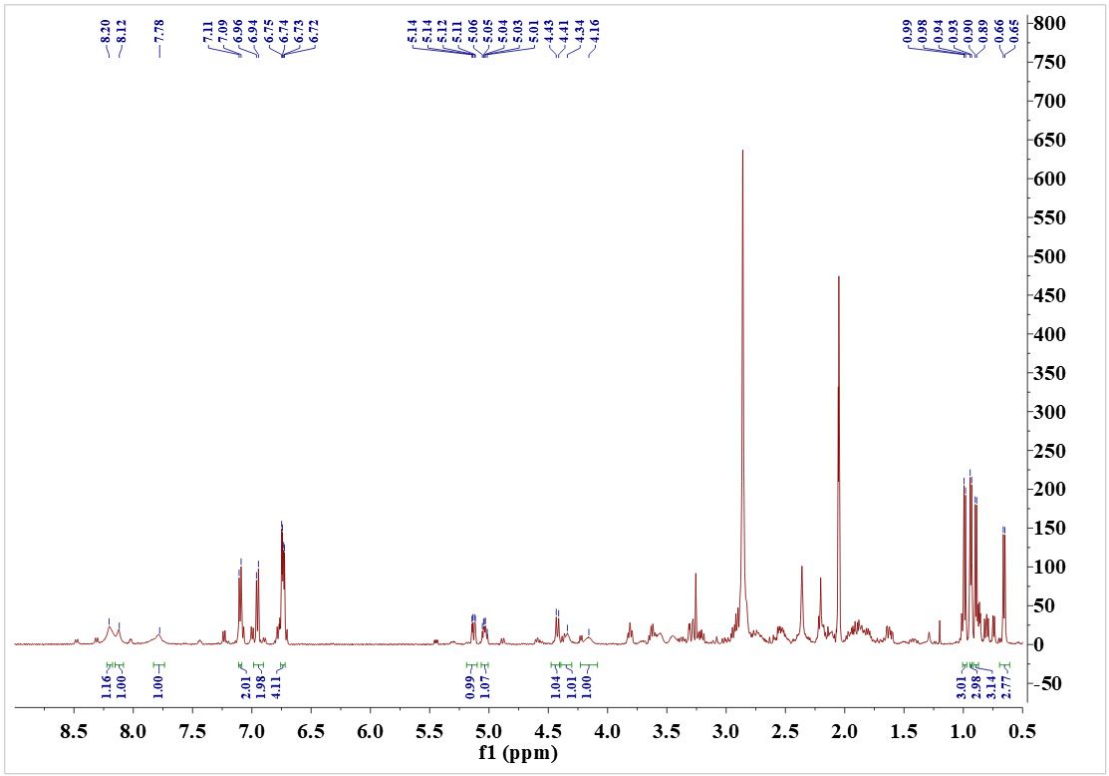

Figure S19. Inhibitory activity of the positive control of 2,4-dichlorophenoxyacetic acid against the radicle growth of *A. retroflexus* seedlings.

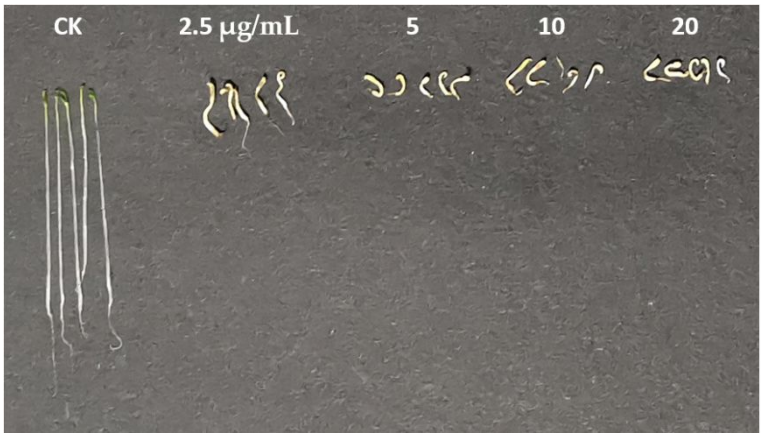

Figure S20. The structures of compound **3** and desmethylisaridin G.

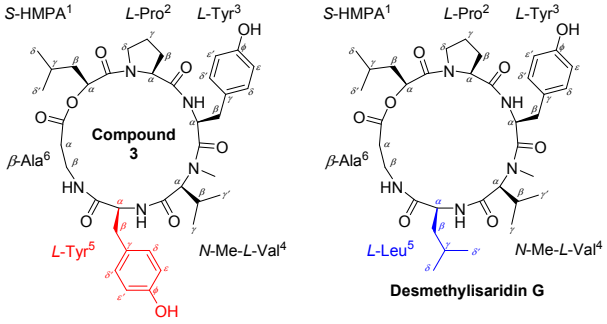

Table S1. Comparison of ^{13}C NMR data of compound **3** and desmethylisaridin G (Acetone-d_6, δ: ppm).

Compound **3**[a]		Desmethylisaridin G[a]		Compound **3**		Desmethylisaridin G	
HMPA		**HMPA**		***N*-Me-Val**		***N*-Me-Val**	
CO	170.1, C	CO	169.1, C	CO	168.8, C	CO	167.9, C
α	73.5, CH	*α*	73.7, CH	*α*	66.7, CH	*α*	66.0, CH
β	39.0, CH_2	*β*	38.1, CH_2	*β*	27.1, CH	*β*	26.2, CH
γ	25.6, CH	*γ*	24.7, CH	*γ*	20.1, CH_3	*γ*	19.1, CH_3
δ	23.4, CH_3	*δ*	22.9, CH_3	*γ′*	19.1, CH_3	*γ′*	18.1, CH_3
δ′	21.8, CH_3	*δ′*	20.9, CH_3	*N*-Me	29.1, CH_3	*N*-Me	28.4, CH_3
Pro^2		**Pro^2**		**Tyr^5**		**Leu^5**	
CO	174.5, C	CO	173.7, C	CO	172.1, C	CO	171.1, C
α	61.5, CH	*α*	61.6, CH	*α*	57.2, CH	*α*	52.1, CH
β	29.0, CH_2	*β*	28.2, CH_2	*β*	39.0, CH_2	*β*	39.5, CH_2
γ	26.5, CH_2	*γ*	25.6, CH_2	*γ*	129.0, C	*γ*	24.5, CH
δ	47.7, CH_2	*δ*	46.9, CH_2	*δ*/*δ′*	130.9, CH	*δ*	22.5, CH_3
Tyr^3		**Tyr^3**		*ε*/*ε′*	116.1, CH	*δ′*	20.6, CH_3
CO	172.8, C	CO	172.2, C	*θ*	156.7, C		
α	50.7, CH	*α*	49.9, CH	***β*-Ala^6**		***β*-Ala^6**	
β	37.9, CH_2	*β*	37.0, CH_2	CO	171.6, C	CO	171.3, C
γ	129.0, C	*γ*	128.0, C	*α*	35.4, CH_2	*α*	34.4, CH_2
δ/*δ′*	131.2, CH	*δ*/*δ′*	130.3, CH	*β*	35.6, CH_2	*β*	34.5, CH_2
ε/*ε′*	116.2, CH	*ε*/*ε′*	115.2, CH				
θ	157.2, C	*θ*	156.3, C				

[a] Both determined in acetone-d_6.

Table S2. Back bone torsion angels (ω) in the crystal structure of **3**.

Amide bonds	Torsion angel (°)
HMPA^1-Pro^2	-7.6
Pro^2-Tyr^3	173.0
Tyr^3-*N*MeVal^4	-3.7
*N*MeVal^4-Tyr^5	179.7
Tyr^5-*β*-Ala^6	-178.7
β-Ala^6-HMPA^1	166.0